ACS APPLIED MATERIALS & INTERFACES

Research Article

www.acsami.org

Consecutive Large-Scale Fabrication of Surface-Silvered Polyimide Fibers via an Integrated Direct Ion-Exchange Self-Metallization Strategy

Enlin Han, Yue Wang, Xue Chen, Gongping Shang, Wenxiao Yu, Hongqing Niu, Shengli Qi,* Dezhen Wu, and Riguang Jin

State Key Laboratory of Chemical Resource Engineering, Beijing University of Chemical Technology, Beijing 100029, People's Republic of China

ABSTRACT: Herein, we report our success on the large-scale online preparation of surface-silver-metallized polyimide (PI) fibers by utilizing silver ammonia complex cation ($[Ag(NH_3)_2]^+$) as the silver (Ag) precursor and pyromellitic dianhydride/4,4′-oxidianiline (PMDA/4,4′-ODA)-based polyimide as the matrix via a direct ion-exchange self-metallization process integrated within a consecutive fiber-spinning procedure. The method works by using the online freshly prepared PMDA/4,4′-ODA-based poly(amic acid) (PAA) fibers as the starting material to perform an ion-exchange reaction in aqueous silver(I) solution to load silver(I) into the PAA precursor fibers, followed by a programmed stepwise thermal treatment process to convert PAA to its final imide form with the concomitant silver(I) reduction and the subsequent aggregation, producing the surface-silvered polyimide hybrid fibers. The influence of thermal cycles on the formation of silver nanostructures, and the variation of surface morphologies and fiber properties during the heating process were investigated. Experimental results indicate that the PI−Ag fibers were produced with good mechanical and thermal properties. In addition, bioassessment suggests that the hybrid fibers exhibit superior antibacterial activities (99.99% in 24 h toward *E. coli*). Outstanding electrical conductive properties of a certain length of the PI−Ag hybrid fiber (electrical resistance: ca. 0.1 Ω cm^{-1}) could also be realized on the composite fibers but with severe destructions in the final mechanical properties. The fibers were also characterized by FTIR, ICP, XRD, SEM, and TEM.

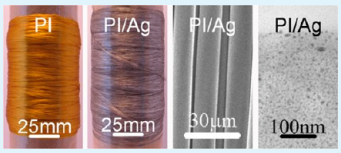

KEYWORDS: *polyimide, silver, fiber, ion exchange*

1. INTRODUCTION

Polyimide (PI) constitutes a class of engineering materials characterized by excellent thermal and mechanical properties, high chemical resistance, low dielectric constant, superior resistance to ultraviolet exposure and nuclear radiation, and good patterning capability.[1−6] As one of the most important derivatives in polyimide family, the polyimide fibers have gained widespread attention for decades in the area of high-performance organic fibers, since they completely inherited all the essential characters of PI and further promoted the performances to considerably higher levels in the fiber form.[7−9] Currently, they have been determined to be attractive materials in many practical applications, including high-temperature dust filter, high-temperature flame-retardant protective clothing, parachutes, electrical insulating materials, cellular structure and sealing materials, composite materials enhancer, and antiradiation materials.[2,9−12]

However, in certain potential applications where functional properties such as catalytic, bio- and electro-properties are required, pure polyimide fibers have shortcomings. To address these deficiencies, combining with metal was considered to be the most effective strategy, and silver was suggested to be one of the best choices for pioneering works, since it possesses excellent electrical, optical, magnetic, catalytic, and bactericidal properties,[13−18] and the silver(I)−silver couple has a favorable standard electrode potential (E_0 = 0.8 V) that allows silver(I) to be readily reduced upon simple heat treatment or ultraviolet illumination.[19−21] Their ideal collaboration was expected to produce surface-silvered polyimide fibers with excellent thermal, mechanical, and various functional properties bearing promising applications in highly active catalysis, antibacteria, sensing, intelligent clothing, medical textile, antistatic electricity, electrical conductivity, radiation, and electromagnetic shielding.

Recently, through the well-developed one-step[7,8] and two-step[12,22−24] spinning techniques, various pure PI fibers with different chemical structures have been successfully prepared in the laboratory.[23−25] However, to date, no works have been reported on the fabrication of surface-silvered polyimide hybrid fibers (i.e., the formation of silver nanostructures on the surface of polyimide fibers, especially in a consecutive large-scale online manner). Whereas, in the past few decades, a variety of methods have been developed for the incorporation of silver nanoparticles into a PI film matrix, including the in situ single-stage self-metallization technique,[19,20,26] the surface-modification self-metallization technique,[1,27−30] and the direct ion-exchange self-metallization technique.[21,31−35] The in situ single-stage self-metallization technique refers to prepare polyimide-silver hybrid materials by thermally treating the poly(amic acid)

Received: February 6, 2013
Accepted: April 17, 2013
Published: April 17, 2013

   dx.doi.org/10.1021/am4005094 | ACS Appl. Mater. Interfaces 2013, 5, 4293−4301

(PAA) precursor doped with silver(I) salts to cycloimidize the PAA into its final PI form with the concomitant thermal reduction of silver(I) and the followed aggregation to yield silver nanoparticles.[19,20,26] Surface-modification self-metallization technique works by using cycloimidized polyimide as the starting material and involves the surface-alkaline-hydrolysis process to cleave the imide ring to alkali polyamate, the ion-exchange process to load Ag ions into the reactive polyamate layer, and the followed thermal curing process to recycloimidize the modified surface polymers and the simultaneous silver(I) reduction to generate silver nanostructures.[1,27−29] The chemistry involved in the direct ion-exchange self-metallization procedure is similar to that of the surface-modification self-metallization route, but with variations by utilizing poly(amic acid) as the beginning.[31,33,34]

Great successes have been achieved on the preparation of surface-silver-metallized polyimide films with these methods.[19,29,30,32,33] However, with the purpose of realizing consecutive online preparation of surface-silver-immobilized polyimide fibers, the surface-modification self-metallization approach is technically inapplicable, since it inevitably includes a long-term alkaline-hydrolysis process and a laborious washing process, both of which are considerably time-consuming and lack efficiency.[29,30] The in situ single-stage self-metallization route is theoretically applicable and was considered in our initial works. However, the poly(amic acid) solution becomes either gelled or too dilute to spinning after the addition of the silver salts, making this method technically inapplicable. Besides, because of the light and air sensitivity of the silver(I) compound, the silver(I)-doped spinning solution would soon become deteriorated, with the observation of distinct color changes over 1−1.5 h after preparation. Furthermore, previous works[19,26] indicate that most of the silver nanoparticles generated with this in situ method are not surface-localized, but distributed in the inner PI matrix, which consequently results in considerably higher silver(I) consumption and low surface-metallization efficiency.

Therefore, in the present work, the direct ion-exchange self-metallization technique was finally employed, which works by using the polyimide precursor (i.e., the poly(amic acid) fibers) as the starting matrix, and then loading silver(I) into the polymer matrix through the ion-exchange reactions of the carboxylic acid groups in PAA macromolecules with Ag ions in aqueous silver(I) precursor solution, followed by thermal treatment to produce the PI−Ag hybrid fibers.[33,34] Scheme 1 shows the overall procedure for the consecutive large-scale online preparation of the surface-silver-metallized PI fibers. Pyromellitic dianhydride/4,4′-oxydianiline (PMDA/4,4′-ODA)-based polyimide was selected in current works due to its large-scale synthetic simplicity; the alkaline silver ammonia complex ($[Ag(NH_3)_2]NO_3$) was chosen as the silver(I) precursor for ion exchange, because of its high efficiency in achieving surface silver metallization of PI films under rather low silver(I) concentration and short ion exchange time, as demonstrated in our previous publications.[33,35] Aqueous $[Ag(NH_3)_2]^+$ solutions with concentrations of 0.010, 0.025, 0.050, and 0.100 M were selected as the Ag ion sources and the ion-exchange time was confined to 30 s to prevent the possible hydrolysis and damaging effect of the alkaline $[Ag(NH_3)_2]^+$ solutions on the polymer matrix during the ion-exchange process. The ideal chemistry involved in the synthesis of the PI−Ag hybrid fibers via the integrated direct ion-exchange self-metallization technique is illustrated in Scheme 2. Experimental results indicate that consecutive large-scale fabrication of surface-silver-metallized polyimide fibers was successfully realized in our works. The present procedure offers advantages of processing simplicity and being cost-effective, since it integrates the fiber-spinning process and the silver-metallization process within one production line, excludes external reducing agents, and requires no extra processing and post-processing. Besides, the entire preparation procedure does not involve any contaminations or pollutional materials, making it environment-friendly and promising strategy for modern industrial production. The obtained polyimide-silver hybrid fibers were characterized by Fourier transform infrared spectroscopy (FTIR), X-ray diffraction (XRD), inductively coupled plasma atomic emission spectroscopy (ICP-AES), scanning electron microscopy (SEM), transmission electron microscopy (TEM), dynamic mechanical analysis (DMA), thermogravimetric analysis (TGA), and antibacterial activity evaluations.

Scheme 1. Illustrative Procedure for the Preparation of Surface-Silvered Polyimide Fibers

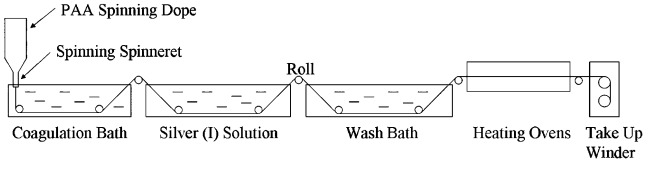

2. EXPERIMENTAL SECTION

2.1. Materials. Pyromellitic dianhydride (PMDA) was provided by Nanjing Lonza, Ltd. and sublimated under vacuum before use. 4,4′-Oxydianiline (4,4′-ODA) was provided by Dongying Guansen Insulation Products Co., Ltd., and recrystallized in ethyl acetate prior to use. Dimethylacetamide (DMAc) was purchased from DuPont Company and used after distillation. Aqueous ammonia solution ($NH_3{\cdot}H_2O$) (analytically pure, 25−28 wt %) was purchased from Beijing Chemical Works. Silver nitrate ($AgNO_3$) (analytically pure, ≥99.8% content) was produced by Beijing Chemical Works and used as received. Silver ammonia complex solutions ($[Ag(NH_3)_2]^+NO_3^-$) were easily prepared by adding dilute ammonia solution dropwise into the aqueous $AgNO_3$ solution until a clear and transparent solution was obtained. Deionized water was used for all aqueous solution preparation.

2.2. Preparation of Surface-Silvered Polyimide Fibers. The synthetic strategy employed for the fabrication of PI−Ag hybrid fibers has been schematically presented in Scheme 2. As the first step, the PMDA/4,4′-ODA PAA solution was prepared by first dissolving the 4,4′-ODA in DMAc followed by the gradual addition of dianhydride with 1 mol % excess. After vigorously stirring in an ice bath for 2−3 h, an amber transparent viscous solution at 20 wt % solid content was finally obtained with an intrinsic viscosity ($[\eta]$) determined to be ∼2.0 dL g^{-1}. The viscous PAA solution was then filtrated and degassed under vacuum at 50 °C to fulfill the followed fiber spinning requirement.

The PAA fibers were then prepared on the wet-spinning production line that has been illustrated in Scheme 1. The temperature of the PAA spinning dope was held constant at 50 °C through a recirculating heater to ensure an appropriate resin fluidity. Under the driving of a constant nitrogen pressure and a proportioning pump (set at 0.2 mL min^{-1}), the PAA solution was extruded through a metal spinneret plate (100 holes, 0.07 mm in diameter) directly into a coagulation bath (1 m in length) filled with pure deionized water, producing a bundle of opalescent primary PAA fibers after solvent release and the subsequent solidification in water. In order to achieve stable and continuous spin filaments, minor stretching (0.5 m min^{-1}) was applied by using a slow

Scheme 2. Schematic Diagram for the Preparation of PI–Silver Composite Fibers via the Integrated Direct Ion-Exchange and Self-Metallization Strategy

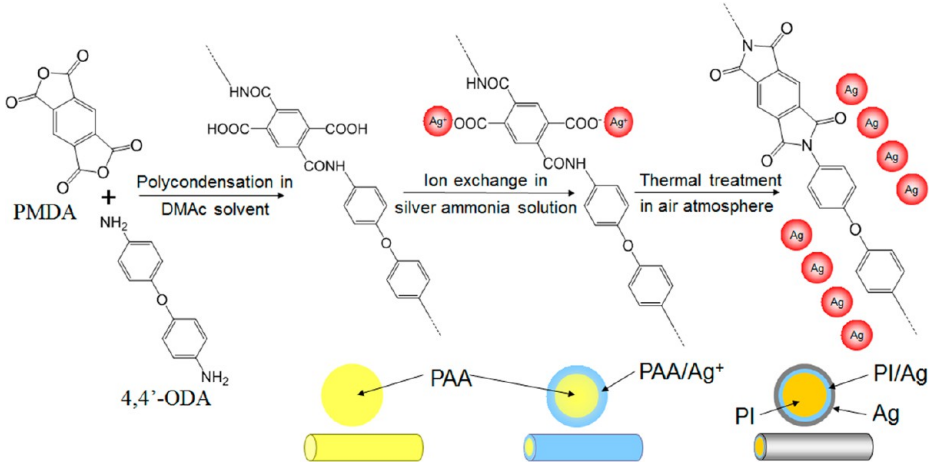

roller speed. Moreover, this spinning speed was kept constant during the entire fiber preparation process.

The obtained PAA fibers were then passed through another bath filled with aqueous silver ammonia solutions to load silver(I) into the PAA fibers through the ion-exchange reactions between the carboxylic acid groups on the PAA macromolecule and the silver ammonia ($Ag[(NH_3)_2]^+$) cations (see Scheme 2). Silver ammonia solution was employed since it has been demonstrated that it is an effective silver source and could achieve higher silver(I) loadings in short period, because of its alkaline nature.[33] The concentration of the silver ammonia solution used in the present work had concentrations of 0.010, 0.025, 0.050, and 0.100 M, respectively. The silver(I)-incorporated PAA fibers were then cleaned under ambient conditions by passing through a followed washing bath filled with deionized water to remove the unreacted free Ag ions. No additional stretching was imposed throughout the entire ion-exchange and washing procedures. Under a constant spinning speed of 0.5 m min^{-1} and a constant bath length of 0.25 m, the ion-exchange time of PAA fibers was determined to be 30 s.

Finally, surface-silvered PI fibers were prepared after passing the silver(I)-doped PAA precursor fibers consecutively through a series of three heating ovens set at 80 °C (1 m in length), 240 °C (2.5 m in length), and 300 °C (2.5 m in length). Because of the length limitation of the heating ovens, the retention times in each oven were 2 min at 80 °C, 5 min at 240 °C, and 5 min at 300 °C. Thermal treatment converts the PAA to its final polyimide form through cyclodehydration with the concomitant silver(I) reduction and subsequent aggregation, yielding surface-silver-nanoparticle-embedded polyimide fibers. No afore-thought tensile loads were performed during the entire thermal treatment process. The final PI–Ag hybrid fibers were collected on a take-up winder and subjected to various measurements.

2.3. Characterization. The intrinsic viscosity ($[\eta]$) measurement was carried out using a Germany Schott 52510 Ubbelohde viscometer with an internal capillary diameter of 0.58 mm. The intrinsic viscosity of the synthesized PAA was determined by first measuring the viscosities of a series of dilute PAA solutions with concentrations of 0.5, 1.0, 1.5, and 2.0 mg mL^{-1}, followed by extrapolating the concentration of the PAA solution to zero, according to eq 1

$$\frac{\eta_{sp}}{c} = [\eta] + k'[\eta]^2 c \quad (1)$$

where η_{sp} is the specific viscosity and c is the concentration, and eq 2

$$\frac{\ln \eta_r}{c} = [\eta] - k''[\eta]^2 c \quad (2)$$

where η_r is the relative viscosity.

The amount of silver(I) loaded into the PAA fibers was quantified with a Seiko Instruments SPS 8000 inductively coupled plasma–atomic emission spectrometry (ICP-AES) system. The measurements were performed after the silver-doped PAA fibers had been dissolved in a 5 wt % nitric acid solution.

Fourier transform infrared (FTIR) spectra of PAA and PI–Ag fibers were collected using a Nicolet Nexus 670 IR spectrometer.

Surface morphologies of the fibers were recorded on a Hitachi S-4700 field-emission scanning electron microscopy (SEM) system that was operating at 20 kV. The samples were coated with ca. 5 nm of platinum prior to measurements. The cross-sectional morphologies of the hybrid fibers were observed using a Hitachi Model H-7650B transmission electron microscopy (TEM) system at an accelerating voltage of 80 kV. Samples for TEM observations were prepared by mounting the ultramicrotome-cut fiber-sectional slices on a carbon-coated copper grid.

X-ray diffraction (XRD) were conducted on a D/Max 2500 VB2+/PC X-ray diffractometer (Rigaku, Tokyo, Japan) in the 5°–90° range at a scanning rate of 10° min^{-1}. The X-ray beam was generated by a Cu Kα target with a wavelength of 0.154056 nm, using a tube voltage of 40 kV and a current of 200 mA.

The electrical resistance was measured using an Agilent 34401A $6_{1/2}$ Digital Multimeter at a constant fiber length of 1 cm.

The thermal mechanical behaviors of the PI and PI/Ag fibers were characterized using a TA Q800 dynamic mechanical analysis (DMA) system under N_2 atmosphere from 30 °C to 500 °C at a heating rate of 3 °C min^{-1}. Thermogravimetric analysis (TGA) was performed with a TA Q50 system (TA Instruments, New Castle, DE) at a heating rate of 10 °C min^{-1} under N_2 and air atmospheres, respectively.

Mechanical properties were evaluated using an YG001A-1 electronic single-fiber-strength measurement system (Taicang Hongda Fangyuan Electric Co., Ltd., China). The drawing speed was 10 mm min^{-1}, and the initial stress was 0.2 cN. The diameters of the prepared fibers were determined by a Motic BA200 optical microscope (Motic China Group Co., Ltd.).

Antibacterial properties were inspected in accordance with Antibacterial Quinn Test method listed in the *Technical Standard for Disinfection* (2002 edition).[46]

3. RESULTS AND DISCUSSION

3.1. Preparation of the PI–Ag Fibers. The ideal chemistry for the fabrication of surface-silvered PI fibers, including the loading of silver(I) via ion exchange, and the cycloimidization of PAA and reduction of silver(I) via thermal treatment, has been depicted in Scheme 2. Because of the presence of many active carboxylic acid groups in the PAA macromolecules, PAAs have significantly higher cation-complexing abilities, compared to their imide forms. This characteristic allows for the in situ reactions of PAA with the

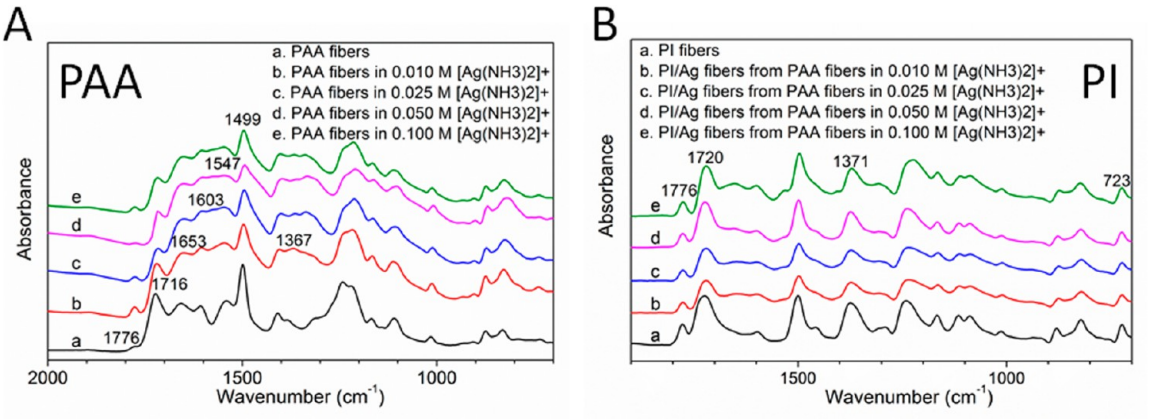

Figure 1. (A) FTIR spectra of the intact PAA fibers (spectrum a) and the silver(I)-doped PAA fibers obtained by ion exchange of the PAA fibers in silver ammonia solutions with different concentrations (spectra b–e) for 30 s. (B) FTIR spectra of the corresponding PI fibers (spectrum a) and PI–Ag hybrid fibers prepared by thermally curing the PAA and silver(I)-doped PAA precursor fibers (spectra b–e) to 300 °C for 300 s.

salts of noble metals having labile anions to generate a metal–polymeric blend.[5,34,36] Based on this, the silver(I) loading was realized in the present work by passing the freshly prepared primary PAA fibers through a bath filled with aqueous silver ammonia solutions with the purpose of performing an ion-exchange reaction between the carboxylic acid groups of PAA and the silver ammonia cations to form a silver polycarboxylate salt (i.e., silver polyamate).

FTIR measurements were performed on the PAA fibers before and after ion exchange, as shown in Figure 1A. The amic acid characteristics of the intact PMDA/4,4′-ODA PAA fibers (see spectrum a in Figure 1A) were indicated by the appearance of three featured absorbance bands, centered at 1716, 1653, and 1547 cm^{-1}, which correspond to the carbonyl stretching vibrations of carboxylic acid, the amide I band (carbonyl stretching), and amide II band (coupling of C–N stretch and N–H deformation), respectively.[34,37] Silver polyamates were verified to be formed in the ion-exchanged PAA fibers, as indicated in spectra b–e in Figure 1A by the observation of a new absorbance bands near 1367 cm^{-1} and the broadening of the absorption peaks near 1603 cm^{-1}, which represent the characteristic absorption of the carboxylate symmetric and asymmetric stretching, respectively.[33,34,38,39]

Silver ammonia complex solution was used as the silver source in current works, since it has been demonstrated that its alkaline nature would significantly enhance the silver(I) loading efficiency,[33,35] i.e., loading a large amount of silver(I) in a short period using considerably dilute aqueous silver(I) solutions. This is considered to be tremendously important for our present consecutive large-scale synthesis of the PI–Ag hybrid fibers, since the length of the fiber production line, particularly the ion-exchange bath, is fixed and limited to be merely 0.25 m, which consequently allows only rather limited silver(I) loading times (as short as 30 s) in current experiments. Nevertheless, as quantified by the Inductively coupled plasma–atomic emission spectroscopy (ICP-AES) measurement, the silver loaded into the PI fibers achieved 1.43, 2.79, 4.38, and 5.41 wt %, respectively, for the PAA fibers ion-exchanged for only 30 s in the corresponding 0.010 M, 0.025 M, 0.050 M, and 0.100 M $[Ag(NH_3)_2]^+$ aqueous solutions, demonstrating the high silver(I) loading efficiencies of the silver ammonia solutions.

Whereas, because of the basic characteristics of the employed silver ammonia complex solution, alkaline hydrolysis was verified to be inevitably occurring on the ion-exchanged PAA fibers, as indicated in spectra b–e in Figure 1A by the observation of the absorbance band broadening at 1653 and 1547 cm^{-1}, and the disappearance of the absorption peak at 1381 cm^{-1} and the appearance of a new broad absorbance band near 1335 cm^{-1}. However, it is believed that, under the present experimental conditions, the basic structural characteristics of the polymer were essentially retained since the overall FTIR spectra were not significantly altered and identical absorption peaks at 1716, 1653, and 1547 cm^{-1} diagnostic of the amic acid features of PAA[37] were all clearly observed in spectra b–e in Figure 1A. This was further confirmed by spectrum a in Figure 1B for the pure PI fibers and spectra b–e in Figure 1B for the PI–Ag hybrid fibers derived from the ion-exchanged PAA precursor fibers, which exhibit basically the same imide vibrations at 1776, 1720, 1371, and 723 cm^{-1}, corresponding to the symmetric and antisymmetric stretching vibrations of the imide carbonyl groups (imide I), the C–N–C axial stretching (imide II), and the out-of-plane bending (imide IV), respectively.[34,37,40]

Thermal treatment of the precursor fibers not only leads to the cycloimidization of PAA into its final PI form but also results in an internal reduction of silver(I) and the consequent aggregation of Ag atoms, as illustrated in Scheme 2, yielding the final silver-doped PI fibers. The reduction of silver(I) was readily occurring upon heating due to its low standard reduction potential (E_0 = 0.80 V).[19−21] Silver aggregation was suggested to be inevitably occurring in the PI–Ag hybrid, because of the poor metal–polymer compatibility and the high surface energies of the naked Ag clusters in atomic or nanometer scale.

Figure 2 shows the cross-sectional TEM morphologies for the PI–Ag hybrid fibers derived from the PAA precursors ion-exchanged for 30 s in 0.010 M, 0.025 M, 0.050 M, and 0.100 M aqueous silver ammonia solutions, respectively. As a reference, TEM images for the pure PI fibers were also presented (Figure 2a). The results clearly indicate that silver-doped PI fibers have been successfully fabricated via our integrated direct ion-exchange self-metallization procedure, as verified in Figure 2b–e by the observation of many randomly distributed spherical silver nanoparticles (NPs). For the PI–Ag fibers prepared by ion exchange in the 0.010 M silver ammonia solution (1.43 wt % silver loading), TEM images in Figure 2b suggest that silver nanoparticles with diameters of ca. 5 nm were formed. Whereas, the silver NPs incorporated in the PI were mainly

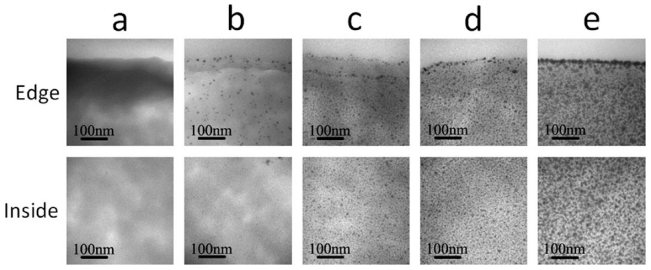

Figure 2. TEM images for (a) the pristine PI fiber and (b–e) the PI–Ag hybrid fibers prepared from the PAA precursors ion-exchanged in aqueous silver ammonia solutions with different concentration for 30 s and then heated to a final temperature of 300 °C for 300 s ((b) 0.010 M, 1.43 wt % silver; (c) 0.025 M, 2.79 wt % silver; (d) 0.050 M, 4.38 wt % silver; and (e) 0.100 M, 5.41 wt % silver).

distributed in the near-surface range and no silver particles were observed in the inner bulk of the hybrid fibers. This is expected since the silver(I) was loaded via ion exchange and the PAA in the outer layer has priority for silver(I) loading. However, when increasing the silver ammonia solution to 0.025 M, TEM images in Figure 2c indicate that the density of the silver nanoparticles in the PI fibers were obviously increased, which is consistent with the increased silver loading (2.79 wt % silver). Furthermore, silver nanoparticles were also presented in the inner bulk of the PI fibers, suggesting the high efficiency of silver ammonia solution at higher concentrations and the occurrence of silver(I) loading across the entire cross-section of the fiber under this experimental condition. Nevertheless, the size of the silver NPs did not exhibit significant alterations, compared to Figure 2b, implying that the silver(I) loading occurring under the present conditions was unsaturated during ion exchange. Further increase in the concentration of the silver ammonia solutions to 0.050 and 0.100 M results in the continued but damped increase in the silver loadings and, consequently, the observation of more silver NPs in the PI fibers, as shown in Figures 2d (4.38 wt % silver loading) and 2e (5.41 wt % silver loading), with the concomitant increase of the size of the silver NPs to ~10 nm. Particularly, a compact surface silver nanolayer was observed to be formed on the PI–Ag hybrid fibers in Figure 2e. Besides, it is interesting to note that, adjacent to the surface silver layer, there is a "near-surface zone", which is ~30–75 nm deep and could be clearly distinguished by the lack of silver NPs. It is suggested that this "depletion zone" was generated by the migration of the silver NPs from the near-surface layer to the outer surface of the fiber. However, the silver NPs below the "depletion zone" did not show any evidence of outward migration, suggesting that the occurrence of silver migration was primarily limited in the near-surface layer.

Figure 3 shows the SEM surface morphologies for the corresponding PI-Ag hybrid fibers in Figure 2. The image in Figure 3a indicates that the pure PI fibers have rather smooth and clean surfaces. Whereas, for the fibers prepared by ion exchange in the 0.010 M aqueous silver ammonia solution and with a silver loading of 1.43 wt %, Figure 3b shows the presence of many small silver nanoclusters on the fiber surfaces, reflecting the successful realization of surface silver immobilization in the current work, consistent with the TEM results observed in Figure 2b. Further increase in silver loadings results in the observation of more Ag NPs and more clear silver aggregations on the fiber surfaces, as displayed in Figures 3c–e. Particularly, at a silver loading of 5.41 wt %, the hybrid fibers

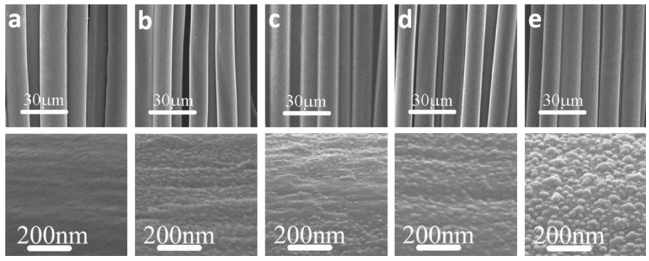

Figure 3. SEM images for (a) the pristine PI fiber and (b–e) the PI–Ag hybrid fibers prepared from the PAA precursors ion-exchanged in aqueous silver ammonia solutions with different concentration for 30 s and then heated to a final temperature of 300 °C for 300 s ((b) 0.010 M, 1.43 wt % silver; (c) 0.025 M, 2.79 wt % silver; (d) 0.050 M, 4.38 wt % silver; and (e) 0.100 M, 5.41 wt % silver).

were prepared with the accumulation of many large silver agglomerations on the outer surfaces, as shown in Figure 3e, which is in good accordance with the observation of a compact surface silver nanolayer in Figure 2e. The results observed here suggest that surface-silver–metallized polyimide fibers have been successfully prepared with the current integrated direct ion-exchange self-metallization strategy. However, electrical resistance measurements indicate that electrical conductivity was not achieved in the PI–Ag hybrid fibers under the present conditions. This is under expectation since Figure 3e indicates that the silver agglomerations are island-like on the fiber surfaces and conductive pathways were visually not formed. Further attempts to prepare electrically conductive PI–Ag fibers were discussed later.

The chemical state of the Ag NPs incorporated within the PI fibers is one of the primary concerns. The four intense peaks detected at 2θ = 38°, 44°, 64°, and 78° on the XRD patterns for the PI–Ag hybrid fibers prepared by ion exchange in the 0.010 M silver ammonia solution, as shown in Figure 4 (same sample

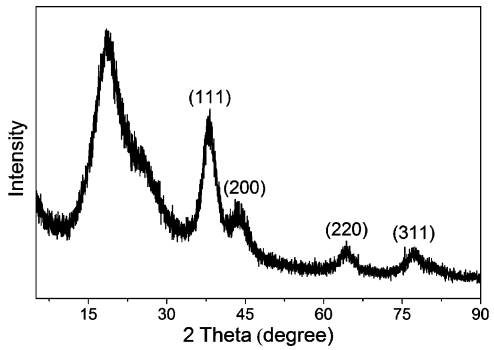

Figure 4. X-ray diffraction (XRD) patterns for the PI–Ag hybrid fibers (1.43 wt % silver loading, using the same sample as that used in Figure 2b) derived from the PAA precursor fibers ion-exchanged in 0.010 M aqueous silver ammonia solution for 30 s and cured at 300 °C for 300 s.

as in Figures 2b and 3b), indicates that the Ag NPs are present in the form of face-centered cubic (FCC) crystallites. The four peaks correspond to the reflections of (111), (200), (220), and (311) crystal faces of FCC silver, respectively. However, they are rather broad, compared to the standard silver reflections, consistent with the particle size of the silver clusters being in the nanometer scope. As estimated by the Scherrer equation,

dx.doi.org/10.1021/am4005094 | ACS Appl. Mater. Interfaces 2013, 5, 4293–4301

$$D_c = \frac{0.89\lambda}{\beta \cos\theta}$$

using the full width at half-maximum (fwhm) of the strongest characteristic reflection (111), the average silver crystallite size was no more than 3.1 nm.[35,36,41,42] Simultaneously, TEM images in Figure 2b exhibit the formation of silver NPs with sizes of ~5 nm, suggesting the occurrence of silver agglomerations during the thermal treatment process.

3.2. Mechanical Properties of the PI–Ag Hybrid Fiber. Table 1 shows the mechanical properties of the prepared PI–Ag hybrid fibers incorporated with different contents of Ag NPs. As can be observed, the pristine polyimide fibers were prepared with a tensile strength of 524.8 ± 28.0 MPa, an initial modulus of 8.27 ± 0.39 GPa, and a percent elongation of 34.76% ± 5.00%. However, the results in Table 1 indicate that the mechanical performances have been considerably destructed after the incorporation of silver particles. For the hybrid fibers prepared after ion exchange in the 0.010 M silver ammonia solution, although only 1.43 wt % silver was loaded into the polyimide matrix, the tensile strength of the hybrid fibers were ~50% compromised, compared to the pure PI fibers. Further increases in the concentration of the silver ammonia solutions result in the continued increase in the silver loadings, as well as the continued degradation in the mechanical properties of the hybrid fibers. In addition, under an aqueous silver ammonia solution of 0.050 M, the tensile strength of the prepared PI–Ag fibers has been destructed to be as weak as 81.7 ± 10.0 MPa. Especially, when increasing the concentration of the silver ammonia solution to 0.100 M, the finally obtained PI–Ag hybrid fibers were becoming considerably brittle and convincing mechanical data could not be measured.

Table 1. Mechanical Properties of the PI–Ag Hybrid Fibers Prepared from the PAA Precursors Ion-Exchanged in Silver Ammonia Solutions of Different Concentration for 30 s and Then Cured to a Final Temperature of 300 °C for 300 s

concentration of silver ammonia solution (M)	silver loading in PI (wt %)	tensile strength (MPa)	initial modulus (GPa)	elongation at break (%)
0.000	0.00	524.8 ± 28.0	8.27 ± 0.39	34.76 ± 5.00
0.010	1.43	267.4 ± 21.0	5.93 ± 0.43	14.10 ± 3.00
0.025	2.79	156.3 ± 20.0	4.38 ± 0.37	2.73 ± 0.50
0.050	4.38	81.7 ± 10.0	3.26 ± 0.30	1.74 ± 0.30
0.100	5.41	*a*		

[a]The fibers could not be tested.

To account for the severe mechanical property destructions observed here, the alkaline hydrolysis occurring on the PAA precursor fibers during their ion exchange in the basic silver ammonia solutions was suggested to be one of the predominant factors. It is assumed that alkaline hydrolysis affects the final properties of the PI fibers in a way that it will cause a serious degradation of the long PAA chains, which would considerably increase the difficulties for the formation of well-defined cycloimidization structures, consequently resulting in the achievement of low imidization degrees upon thermal treatment. Although FTIR measurements displayed almost the same spectroscopic characteristics for the pure PI fibers and the PI–Ag hybrid fibers with different ion-exchange history, as shown in Figure 1B, quantitative evaluations on the FTIR spectra indicates that the absorbance peak intensity ratios, I_{1371}/I_{1497}, which could be utilized to characterize the degree of cycloimidization,[40] gradually decreased from 1.204 for the pure PI fibers to 0.901, 0.740, 0.711, and 0.693 for the PI–Ag hybrid fibers with respective ion-exchange histories of 0.010, 0.025, 0.050, and 0.100 M silver ammonia solutions for 30 s. As expected, ion exchange in higher concentrated silver ammonia solutions (also higher basicity) results in the realization of lower imidization degrees in the final PI–Ag fibers, confirming the above-mentioned alkaline-hydrolysis-related assumption, and accounting for the observed destructions in mechanical properties of the hybrid fibers. Besides, the catalytic and oxidative degradation effect of the silver particles on the polymer matrix during high-temperature thermal treatment process, as reported in the literatures,[19,33,43] was suggested to be another important reason responsible for the observed destruction of the mechanical performances of the hybrid fibers.

3.3. Thermal Behavior. To evaluate the thermal behavior of the silver-doped hybrid fibers, dynamic mechanical thermal analysis was conducted on the PAA, PI, and PI–Ag fibers, respectively, the results of which are shown in Figure 5. The DMA tan δ curves provide more useful information. As displayed, two major loss peaks centered at ~210 and 398 °C were clearly presented on the tan δ curves for the PAA precursor fibers (Figure 5a), which should be ascribed to the plasticization and cyclization of PAA, and the glass transition of the polyimide chains, respectively, consistent with the concomitant observation of two distinct drops in the storage modulus. However, for the PI fibers prepared in our current work, as shown on the tan δ curve in Figure 5b, only one major peak at ~408 °C, indicative of the polyimide glass transition, was observed. And, the tan δ loss peak at ca. 210 °C was completely disappeared in Figure 5b, suggesting that the PAAs have been fully converted into their imide form under the thermal treatment procedures employed in our current work. Besides, Figure 5b shows that the glass-transition temperature of our prepared PI fibers was obviously higher (ca. 10 °C) than that observed in the DMA thermal curing profiles for the PAA fibers in Figure 5a (398 °C). This is somewhat unexpected and might be explained by the fact that our PI fibers were prepared by thermal cycloimidization under directional drawing, which might result in the formation of more-compact imide structures and, consequently, the enhanced glass-transition temperature. Similarly, for the PI–Ag hybrid fibers, only the loss peak for the glass transition of polyimide was presented on the tan δ curve, as can be seen in Figure 5c. However, the transition temperature exhibits significant deviations from the pure PI

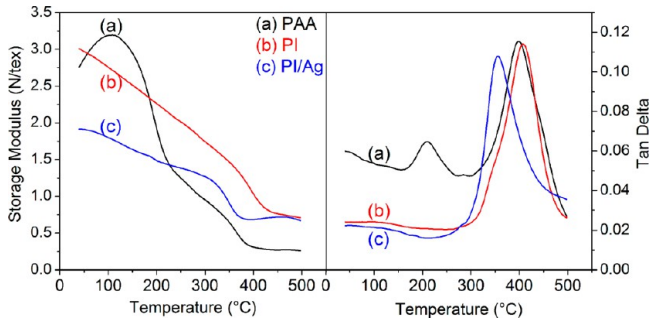

Figure 5. DMA storage modulus and tan δ curves versus temperature for the (a) PAA fibers, (b) PI fibers cured to 300 °C for 300 s, and (c) PI–Ag fibers that were obtained after ion exchange in 0.010 M silver ammonia solution for 30 s and then heated to 300 °C for 300 s.

fibers and reduces to be 355 °C. The result observed here indicates that the incorporation of silver has substantially affected the imidization process of the polymer matrix and resulted in the formation of deficient polyimide structures, consistent with the previously observed degradations in the mechanical performances of the hybrid fibers.

Table 2 shows the thermogravimetric analysis results for the pure PI fibers and PI−Ag hybrid fibers prepared under different

Table 2. T_{d5} and T_{d10} Data in Nitrogen Atmosphere and Air Atmosphere for the Pristine PI Fibers, and the PI−Ag Hybrid Fibers Prepared from the PAA Fibers That Were Ion-Exchanged with Silver Ammonia Solutions with Different Concentrations for 30 s and Then Heated to 300 °C for 300 s

		Nitrogen Atmosphere		Air Atmosphere	
$[Ag(NH_3)_2]^+$ concentration (M)	silver loading in PI (wt %)	T_{d5} (°C)	T_{d10} (°C)	T_{d5} (°C)	T_{d10} (°C)
0.000	0.00	566	579	506	536
0.010	1.43	563	578	390	397
0.025	2.79	566	585	381	386
0.050	4.38	543	582	363	377
0.100	5.41	512	570	356	366

ion exchange conditions. The pure PI fibers exhibit considerably excellent thermal stabilities in both nitrogen and air environments, with the 10%-weight-loss temperatures as high as 579 and 536 °C in nitrogen and air, respectively. However, the incorporation of silver into the PI fiber has significantly diminished its high-temperature thermal stabilities, as observed in Table 2. Although, under nitrogen atmosphere, the 10%-weight-loss temperatures of the hybrid fibers are almost the same as that for the pure polyimide fiber, in air, there is a considerably large reduction in thermal stability, with the temperature of 10% weight loss being 139−170 °C, which is decreased compared to that of the pure PI. Also, it is observed that higher silver loadings cause more serious degradations in the thermal stability of the fibers. This is expected since silver particles have a significant catalytic and oxidative decomposition effect on the polyimide matrix at a high temperature, especially in nanometer scale, as reported in the literature.[1] Nevertheless, with the lowest 10%-weight-loss temperature being >360 °C, the stability of the silver-doped fibers prepared in our current work are also in the class of high-temperature materials and could still meet the requirements for many high-temperature applications.

3.4. Antibacterial Property Assessment. Silver has been known to have excellent antibacterial properties for many years.[14,15,18,44,45] Because of this, our silver-doped PI fibers were also suggested to be promising materials in the antibacterial field, since the silver is present in nanometer scale and the PI fibers are biocompatible and possess relatively large surface areas. As a potential application, bioassessment was carried out on our prepared PI−Ag hybrid fibers by using the gram-negative bacterium *E. coli* as the target, the results of which were shown in Figure 6. As can be observed in the control of Figure 6, the pure PI fibers do not show any discernible influence on the growth and reproduction of the bacterial strain and numerous living bacterial strains were observed after contacting with the PI fibers for 24 h. Whereas, for the silver-doped PI fibers, as can be observed in Figure 6 (sample), the

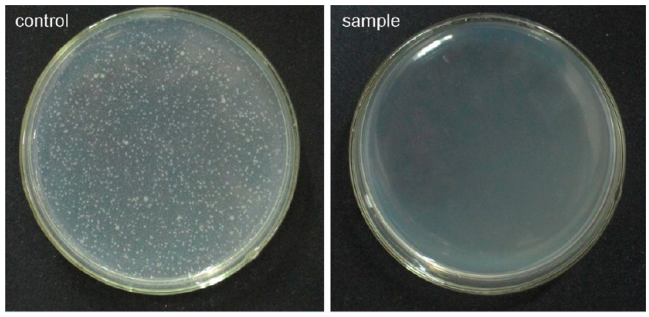

Figure 6. Photographs of *E. coli* colonies incubated on agar plates obtained from cultivated suspensions in the presence of pure PI fibers (control) and 1.43-wt %-silver-doped PI fibers (sample) (0.5 g fibers in 50 mL cultivated suspensions).

concentration of the *E. coli* bacteria colonies was reduced from 4.56×10^6 cfu mL^{-1} to almost 0 during the 24 h of contact with the hybrid fibers, indicating the high antibacterial activity (99.99% in 24 h) of the prepared PI−Ag hybrid fibers.

3.5. Attempt To Prepare Electrically Conductive PI−Ag Fibers. Although Ag NPs could be successfully incorporated into the PI matrix via our integrated direct ion-exchange self-metallization process and the PI−Ag fibers could be prepared in large scale, it should be noted that no electrical conduction was realized under the current preparation conditions. This is assumed to be due to the insufficient silver aggregation and the formation of in-continuous surface silver layers, as observed in Figure 3. In addition, the short high-temperature treatment time (i.e., at 300 °C for 300 s) employed during the online consecutive production was suggested to one of the key reasons. Therefore, the online-prepared PI−Ag hybrid fibers were further heated to 0.5, 1, 1.5, and 2 h at 300 °C with the attempt to achieve electrical conduction. Table 3 lists the electrical resistance data recorded for the PI−Ag hybrid fibers heated to different thermal stages.

Table 3. Electrical Resistance Data for the PI−Ag Hybrid Fibers Prepared by Ion Exchange in Silver Ammonia Solutions with Different Concentration and Then Cured for Different Times at 300 °C[a]

		Resistance after Heating at 300 °C (Ω cm^{-1})			
$[Ag(NH_3)_2]^+$ concentration (M)	silver loading in PI (wt %)	0.5 h	1 h	1.5 h	2 h
0.100	5.41	1.3	0.5	0.3	0.2
0.050	4.38	NC	NC	30.0	15.0
0.025	2.79	NC	NC	NC	NC
0.010	1.43	NC	NC	NC	NC

[a]NC = not conductive.

The results indicate that, for the PI−Ag hybrid fibers prepared via ion exchange in the 0.010 and 0.025 M silver ammonia solutions, electrical conduction could not be realized by extending the thermal treatment time to 2 h, which is probably due to the low silver loadings in the polymer matrix (i.e., 1.43 and 2.79 wt % silver). However, the PI−Ag hybrid fibers (4.38 wt % silver loading) prepared by ion exchange in the 0.050 M silver ammonia solution turned out to be conductive after heating at 300 °C for 1.5 h. In addition, an electrical resistance of 30 Ω cm^{-1} was realized on the fibers and

dx.doi.org/10.1021/am4005094 | ACS Appl. Mater. Interfaces 2013, 5, 4293−4301

soon reduced to 15 Ω cm^{-1} after further heating to 2 h. The hybrid fibers (5.41 wt % silver) prepared by ion exchange in the 0.100 M silver ammonia solution immediately became conductive after heating to 300 °C for 0.5 h, with the achievement of an electrical resistance of 1.3 Ω cm^{-1}, which were further decreased to be comparable to pure silver metal with increased heating time.

SEM surface morphologies for the pure PI and PI−Ag hybrid fibers with different silver contents prepared by heating to 300 °C for 1.5 h are shown in Figure 7. The pure PI fibers in Figure 7a without any silver dopant exhibit smooth and bald outer surfaces. Similar smooth surface morphologies are also observed in Figure 7b for the hybrid fibers with 1.43 wt % silver content. The SEM image at higher magnification reveals the scattering of many island-like Ag NPs on the fibers. It is clear that the amount of silver particles is far from enough to cover the surface region, so conductivity is not detected. The surface morphology of the hybrid fibers exhibits significant alterations when prepared by ion exchange in the 0.025 M silver ammonia solution, as shown in Figure 7c. The fiber became considerable rough with the appearance of many large silver agglomerations on the surface, implying the occurrence of considerable silver aggregations. However, conductivity was still not achieved on the fibers since the silver agglomerations are observed to be isolated from each other and conductive path was not formed. Further increase in the silver loadings results in the formation of net-like conductive paths on the surface of the hybrid fibers (4.38 wt % silver), as displayed in Figure 7d, accounting for the good electrical condutive properties (electrical resistance: 30 Ω cm^{-1}). Figure 7e shows that, for the PI−Ag hybrid fibers (5.41 wt % silver) prepared by ion exchange in the 0.100 M silver ammonia solution, the surface of the hybrid fibers has been completely covered by continuous and compact silver layers. Therefore, electrical conduction comparable to pure silver metal was realized. Unfortunately, it should be mentioned and emphasized that once electrical conductivity was achieved, the prepared PI−Ag fibers will become considerably brittle. The main reason might lie in the highly rigid molecular structures of the PMDA/ODA-based polyimide, which was suggested to be sensitive to alkaline hydrolysis and Ag-NP-catalyzed thermo-oxidative degradation.

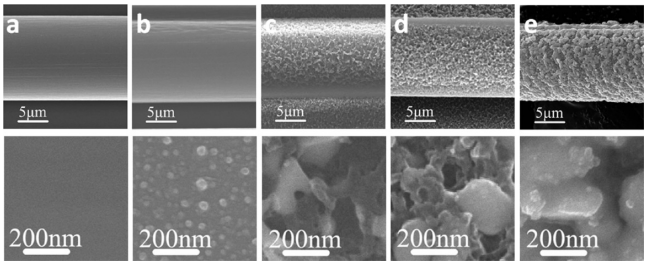

Figure 7. SEM images for (a) the pure PI fibers and (b−e) the PI−Ag hybrid fibers fibers prepared by ion exchange in the (b) 0.010 M, (c) 0.025 M, (d) 0.050 M, and (e) 0.100 M aqueous silver ammonia solutions for 30 s and then heated to 1.5 h at 300 °C.

4. CONCLUSIONS

Consecutive large-scale preparation of silver-doped polyimide (PI) fibers was realized in the present work via the integrated direct ion-exchange self-metallization procedure. By employing PMDA/ODA-based polyimide as the matrix and aqueous silver ammonia solution as the silver precursor, PI−Ag hybrid fibers with good mechanical performances were fabricated, but the concentration of the silver ammonia solution used for silver loading must be strictly limited to be in 0.025 M to limit the damaging effect on the polymer matrix. The incorporation of silver nanoparticles (Ag NPs) has substantially affected the imidization structures and thermal stabilities of the PI fibers. Whereas, the PI−Ag hybrid fibers still exhibit a 10%-weight-loss temperature over 570 °C in nitrogen and 366 °C in air, which could still meet many high-temperature applications. Bioassessment demonstrates that our prepared PI−Ag hybrid fiber has outstanding antibacterial activity against *E. coli* colonies (99.99% in 24 h), implying its potential as a promising antibacterial material. Excellent electrical conductive property could also be achieved on the hybrid fibers by simply extending the high-temperature thermal treatment time. However, this always causes disastrous destructions in the mechanical properties. Nonetheless, inexpensive and efficient synthetic pathways now exist to prepare metal-nanoparticle-doped PI fibers in consecutive large scale.

AUTHOR INFORMATION

Corresponding Author

*Tel.:+86 10 6442 4654. Fax: +86 10 6442 1693. E-mail: qisl@mail.buct.edu.cn.

Notes

The authors declare no competing financial interest.

ACKNOWLEDGMENTS

The authors acknowledge financial supports from the National Natural Science Foundation of China (NSFC, Grant Nos. 50903006 and 51071015) and the Specialized Research Fund for the Doctoral Program of Higher Education (SRFDP, Project No. 20090010120008).

REFERENCES

(1) Akamatsu, K.; Shinkai, H.; Ikeda, S.; Adachi, S.; Nawafune, H.; Tomita, S. *J. Am. Chem. Soc.* **2005**, *127*, 7980−7981.
(2) Neuber, C.; Schmidt, H. W.; Giesa, R. *Macromol. Mater. Eng.* **2006**, *291*, 1315−1326.
(3) Zhang, J.; Sullivan, M. B.; Zheng, J. W.; Loh, K. P.; Wu, P. *Chem. Mater.* **2006**, *18*, 5312−5316.
(4) Li, T. L.; Hsu, S. L. C. *J. Phys. Chem. B* **2010**, *114*, 6825−6829.
(5) Carlberg, B.; Ye, L. L.; Liu, J. *Small* **2011**, *7*, 3057−3066.
(6) Yuan, W.; Che, J.; Chan-Park, M. B. *Chem. Mater.* **2011**, *23*, 4149−4157.
(7) Cheng, Z. D. S.; Wu, Z.; Mark, E.; Hsu Steven, L. C.; Harris Frank, W. *Polymer* **1991**, *32*, 1803−1810.
(8) Eashoo, M.; Shen, D.; Wu, Z.; Lee, C. J.; Harris, F. W.; Cheng, S. Z. D. *Polymer* **1993**, *34*, 3209−3215.
(9) Zhang, Q. H.; Dai, M.; Ding, M. X.; Chen, D. J.; Gao, L. X. *J. Appl. Polym. Sci.* **2004**, *93*, 669−675.
(10) Liu, X.; Gao, G.; Dong, L.; Ye, G.; Gu, Y. *Polym. Adv. Technol.* **2009**, *20*, 362−366.
(11) Wang, Q.; Zhang, X.; Pei, X. *Mater. Des.* **2010**, *31*, 3761−3768.
(12) Xiang, H.; Chen, L.; Hu, Z. *Polym. Bull.* **2011**, 40−50.
(13) Son, W. K.; Youk, J. H.; Lee, T. S.; Park, W. H. *Macromol. Rapid Commun.* **2004**, *25*, 1632−1637.
(14) Panáček, A.; Kvítek, L.; Prucek, R.; Kolář, M.; Večeřová, R.; Pizúrová, N.; Sharma, V. K.; Nevěčná, T. j.; Zbořil, R. *J. Phys. Chem. B* **2006**, *110*, 16248−16253.
(15) Kong, H.; Jang, J. *Langmuir* **2008**, *24*, 2051−2056.
(16) Merga, G.; Cass, L. C.; Chipman, D. M.; Meisel, D. *J. Am. Chem. Soc.* **2008**, *130*, 7067−7076.

(17) Severin, N.; Kirstein, S.; Sokolov, I. M.; Rabe, J. P. *Nano Lett.* **2009**, *9*, 457−461.
(18) Xiu, Z. M.; Zhang, Q. B.; Puppala, H. L.; Colvin, V. L.; Alvarez, P. J. J. *Nano Lett.* **2012**, *12*, 4271−4275.
(19) Southward, R. E.; Stoakley, D. M. *Prog. Org. Coat.* **2001**, *41*, 99−119.
(20) Southward, R. E.; Thompson, D. W. *Mater. Des.* **2001**, *22*, 565−576.
(21) Qi, S. L.; Wu, D. Z.; Bai, Z. W.; Wu, Z. P.; Yang, W. T.; Jin, R. G. *Macromol. Rapid Commun.* **2006**, *27*, 372−376.
(22) Zhang, Q. H.; Dai, M.; Ding, M. X.; Chen, D.; Gao, L. X. *Eur. Polym. J.* **2004**, *40*, 2487−2493.
(23) Liu, X.; Pan, R.; Xu, W.; Ye, G.; Gu, Y. *Polym. Eng. Sci.* **2009**, *49*, 1225−1233.
(24) Niu, H.; Qi, S.; Han, E.; Tian, G.; Wang, X.; Wu, D. *Mater. Lett.* **2012**, *89*, 63−65.
(25) Gao, G.; Dong, L.; Liu, X.; Ye, G.; Gu, Y. *Polym. Eng. Sci.* **2008**, *48*, 912−917.
(26) Qi, S. L.; Wu, D. Z.; Wu, Z. P.; Wang, W. C.; Jin, R. G. *Polymer* **2006**, *47*, 3150−3156.
(27) Akamatsu, K.; Ikeda, S.; Nawafune, H. *Langmuir* **2003**, *19*, 10366−10371.
(28) Wu, Z. P.; Wu, D. Z.; Qi, S. L.; Zhang, T.; Jin, R. G. *Thin Solid Films* **2005**, *493*, 179−184.
(29) Wu, Z.; Wu, D.; Yang, W.; Jin, R. *J. Mater. Chem.* **2006**, *16*, 310−316.
(30) Yang, S.; Wu, D.; Qi, S.; Cui, G.; Jin, R.; Wu, Z. *J. Phys. Chem. B* **2009**, *113*, 9694−9701.
(31) Qi, S.; Wu, Z.; Wu, D.; Wang, W.; Jin, R. *Langmuir* **2007**, *23*, 4878−4885.
(32) Qi, S.; Wu, Z.; Wu, D.; Wang, W.; Jin, R. *Chem. Mater.* **2007**, *19*, 393−401.
(33) Qi, S.; Wu, Z.; Wu, D.; Jin, R. *J. Phys. Chem. B* **2008**, *112*, 5575−5584.
(34) Qi, S.; Wu, Z.; Wu, D.; Yang, W.; Jin, R. *Polymer* **2009**, *50*, 845−854.
(35) Han, E.; Wu, D.; Qi, S.; Tian, G.; Niu, H.; Shang, G.; Yan, X.; Yang, X. *ACS Appl. Mater. Interfaces* **2012**, *4*, 2583−2590.
(36) Andreescu, D.; Wanekaya, A. K.; Sadik, O. A.; Wang, J. *Langmuir* **2005**, *21*, 6891−6899.
(37) Pramoda, K. P.; Liu, S.; Chung, T. S. *Macromol. Mater. Eng.* **2002**, *287*, 931−937.
(38) Thomas, R. R.; Buchwalter, S. L.; Buchwalter, L. P.; Chao, T. H. *Macromolecules* **1992**, *25*, 4559−4568.
(39) Okumura, H.; Takahagi, T.; Nagai, N.; Shingubara, S. *J. Polym. Sci., Polym. Phys.* **2003**, *41*, 2071−2078.
(40) Suzuki, Y.; Maekawa, Y.; Yoshida, M.; Maeyama, K.; Yonezawa, N. *Chem. Mater.* **2002**, *14*, 4186−4191.
(41) Kalishwaralal, K.; Deepak, V.; Ramkumarpandian, S.; Nellaiah, H.; Sangiliyandi, G. *Mater. Lett.* **2008**, *62*, 4411−4413.
(42) Shin, Y.; Bae, I.-T.; Arey, B. W.; Exarhos, G. J. *J. Phys. Chem. C* **2008**, *112*, 4844−4848.
(43) Zhang, F.; Guan, N.; Li, Y.; Zhang, X.; Chen, J.; Zeng, H. *Langmuir* **2003**, *19*, 8230−8234.
(44) Wang, Q.; Yu, H.; Zhong, L.; Liu, J.; Sun, J.; Shen, J. *Chem. Mater.* **2006**, *18*, 1988−1994.
(45) Abdullayev, E.; Sakakibara, K.; Okamoto, K.; Wei, W.; Ariga, K.; Lvov, Y. *ACS Appl. Mater. Interfaces* **2011**, *3*, 4040−4046.
(46) *Technique Standard For Disinfection*; Ministry of Health of People's Republic of China: Beijing, 2002.